A Model for Switching Traps in Amorphous Oxides

Wolfgang Goes*, Tibor Grasser*, Markus Karner*, and Ben Kaczer°
*Christian Doppler Laboratory for TCAD at the Institute for Microelectronics, TU Wien, Gußhausstraße 27–29/E360, A-1040 Wien, Austria
Email: {goes|grasser|karner}@iue.tuwien.ac.at
°IMEC, Kapeldreef 75, B-3001 Leuven, Belgium
Email: kaczer@imec.be

***Abstract*—Negative Bias Temperature Instability (NBTI) is frequently suspected to arise from a delicate interplay between some sort of hole trapping and an interface generation mechanism. In a recently suggested model the E' center along with its second form as an $\mathrm{Si}-\mathrm{Si}$ dimer are supposed to play a key role. Despite of its successful application to a large amount of experimental data, this model relies on a classical determination of the bandedge energy diagram and the carrier concentrations. The occurrence of subbands in the inversion layer shifts the initial energy level for charge trapping and may thus strongly impact the trapping dynamics. We evaluate the new model against measurement data in order to investigate the impact of quantization effects on the model parameters.**

I. Introduction

Negative Bias Temperature Instability (NBTI) still ranks among the most serious reliability issues in present-day semiconductor devices. Even though a series of models have been devised to explain NBTI, none of them have so far been capable of reproducing the experimentally observed touchstones, such as the field- and temperature-dependence as well as the asymmetry between stress and relaxation. A recently proposed mechanism [1], involving charge trapping according to lattice relaxation multiphonon emission (LRME), seems to overcome these difficulties. The model relies on the well-established picture of switching traps, as reported from electron spin resonance measurements [2]. Here, a rare trapping event triggers a defect precursor (Si dimer) to form an active defect (E' center). In this new configuration, the time constants for trapping and detrapping events are drastically reduced.

This is reminiscent of another intensively studied reliability issue — namely, random telegraph noise (RTS), where charge trapping is also assumed to proceed via LRME. Thorough investigations have shown classical calculations to be oversimplified and especially stressed the strong impact of quantization in the inversion layer on trapping dynamics [3, 4]. Hence, we extend the model by including quantum confinement and the impact of bound states on the trapping behavior.

II. Modeling

In our model the defect precursor is a neutral $\mathrm{Si}-\mathrm{Si}$ dimer configuration (state 1, cf. Fig. 1) which features an electron level far below the silicon valence band edge. This defect can capture a hole which causes the rupture of the dimer bond and results in structural relaxation. While one of the silicon atoms takes the positive charge and relaxes backwards to establish a weak bond to a nearby oxygen atom, the other silicon atom carries a dangling bond (state 2). The dangling bond (E' center) with an energy level close to the silicon band gap is capable of trapping or detrapping charge carriers from the silicon substrate. This repeated exchange of charge carriers with the substrate is reflected in switching back and forth between state 2 and 3. In its neutral charge state, it also may return back to its initial configuration by surmounting a thermal barrier. Alternatively, the defect in state 2 may undergo a reaction with the hydrogen attached to the final complex.

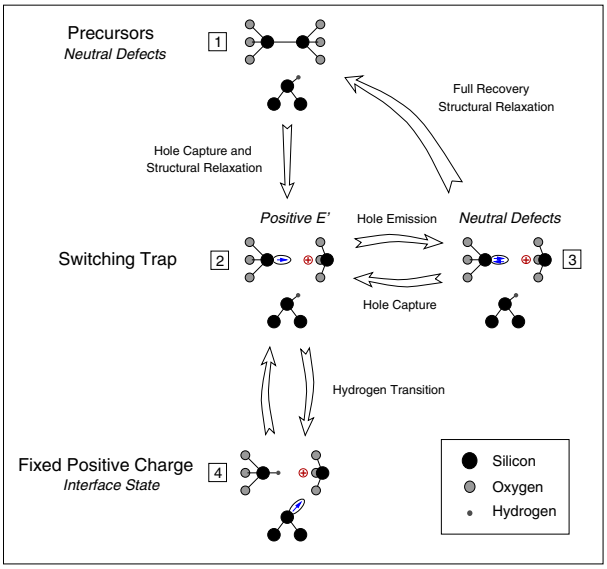

Fig. 1. Schematic representation of switching traps as suggested in [2]: State 1 depicts the precursor state, the $\mathrm{Si}-\mathrm{Si}$ bond. The transition from state 1 to state 2 proceeds via hole capture followed by the subsequent break-up of the $\mathrm{Si}-\mathrm{Si}$ bond and a structural relaxation to the E' center configuration. The positive charge can either be locked in the defect via a H reaction to state 4 or it can be annihilated by electron capture (state 3). For the latter case, two electrons reside at the Si dangling bond and the way back to state 1 is enabled by overcoming a thermal barrier.

On the basis of this picture, trapping dynamics are described by the following set of rate equations

$$\partial_t f_1 = -f_1 k_{12} + f_3 k_{31}, \tag{1}$$
$$\partial_t f_2 = +f_1 k_{12} - f_2 k_{23} + f_3 k_{32} - f_2 k_{24} + f_3 k_{42}, \tag{2}$$
$$\partial_t f_3 = +f_2 k_{23} - f_3 k_{32} - f_3 k_{31}, \tag{3}$$
$$\partial_t f_4 = +f_2 k_{24} - f_4 k_{42} \tag{4}$$

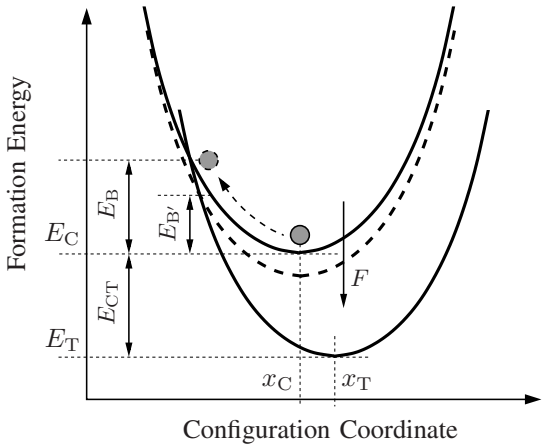

Fig. 2. Schematic representation of the LRME process: E_{C} and E_{T} are referred to as the formation energies of the entire system when the electron is situated either in the conduction band or in the trap. The corresponding configuration coordinates for their equilibrium positions are denoted as x_{C} and x_{T}. The parabola indicate the energy increase due to thermally induced distortions of the defect. According to MPFAT theory, the parabola is moved downwards upon application of an electric field F and thus the intersection point ($E_{\mathrm{B}'}$) is considerably lowered. Mind that the overall barrier for a transition in the forward direction is E_{B} while it consists of $E_{\mathrm{CT}} + E_{\mathrm{B}}$ for the reverse direction, using the shorthand $E_{ij} = E_i - E_j$.

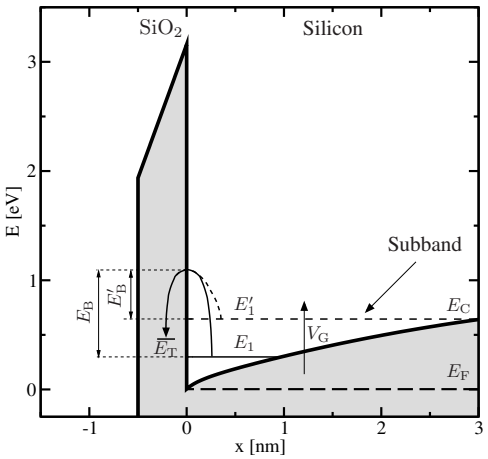

Fig. 3. Schematic of the LRME trapping process regarding quantization in the inversion layer. According to classical considerations, the electrons involved in LRME tunneling come from the conduction band edge E_{C} as computed by a Poisson solver for instance. In the quantum mechanical analogy, the lowest subband carries most of conduction band electrons and thus serves as the source of electrons for the LRME process. However, this subband is shifted upwards from E_1 to E'_1 when the gate voltage V_{G} is raised. As a consequence, the energy barrier E_{B} for the LRME transition is decreased to E'_{B}. The position of the trap level as well as the LRME barrier have exponential dependences and thus are quite sensitive to changes in these quantities.

with the constraint

$$1 = f_1 + f_2 + f_3 + f_4, \tag{5}$$

where f_i corresponds to the occupation of the state i in Fig. 1 and k_{ij} denotes the transition rates from state f_i to state f_j. Hole trapping into the precursor state (k_{12}) is assumed to follow LRME theory [5]. The tunneling dynamics of the E' center is reflected in the rates k_{23} and k_{32} and is also described by LRME theory. The rate k_{31} accounts for the possibility of the neutralized E' center to collapse to its dimer configuration via thermal activation over a large barrier.

While the conventional concept of elastic tunneling rests upon the assumption that the initial electron level must coincide with the final defect level, LRME theory [5, 6] solely accounts for the total energy conservation of the entire system including both the substrate and the dielectric. As illustrated in Fig. 2, the defect acquires just as much thermal energy in form of lattice distortions so that the total energy before and after the tunneling transition is preserved. This is the case when the system is found at the intersection point of the solid curves in Fig. 2. For a tunneling transition of the electron from the substrate conduction band into the trap, the system has to surmount an energy barrier E_{B}. For the reverse direction, the energy barrier is increased by E_{CT}.

The transition rates k_{12}, k_{23} and k_{32} read:

$$k_{\mathrm{f,n}} = n\,\sigma_{\mathrm{n}}\,v_{\mathrm{n}}^{\mathrm{th}}\,\mathrm{e}^{-\beta E_{\mathrm{B}}}\,\Theta(E_{\mathrm{TC}}, \mathrm{e}^{-\beta E_{\mathrm{TC}}}, 1), \tag{6}$$

$$k_{\mathrm{r,n}} = n\,\sigma_{\mathrm{n}}\,v_{\mathrm{n}}^{\mathrm{th}}\,\mathrm{e}^{-\beta E_{\mathrm{B}}}\,\Theta(E_{\mathrm{TC}}, \mathrm{e}^{-\beta E_{\mathrm{FC}}}, \mathrm{e}^{-\beta E_{\mathrm{FT}}}), \tag{7}$$

using the auxiliary function

$$\Theta(E_{\mathrm{switch}}, a, b) = \begin{cases} a & E_{\mathrm{switch}} \geq 0 \\ b & E_{\mathrm{switch}} < 0 \end{cases} \tag{8}$$

and the abbreviation $\beta = 1/k_{\mathrm{B}}T$. E_{C} and E_{T} is the formation energy when the electron is in the substrate conduction band or in the trap state, respectively. E_{F} refers to the substrate Fermi level at the interface according to the assumption that the traps located close to the interface are controlled by the substrate Fermi level. n and v^{th} denote the electron concentration and their thermal velocity, respectively. The capture cross section σ_{n} includes the tunneling probability, modeled by a simple WKB approximation $\sigma_{\mathrm{n},0} \exp\big(-x/x_{\mathrm{n},0}\big)$. Analogous rate equations hold for hole trapping [1]. According to multi-phonon field-assisted tunneling (MPFAT) theory [7], a field-enhancement factor of the form $\mathrm{e}^{(F/F_{\mathrm{c}})^2}$ is introduced in the above equations, where F stands for the electric field within the dielectric and F_{c} denotes a reference field.

The remaining transitions are thermally activated as follows:

$$k_{31} = \nu_1\,\mathrm{e}^{-\beta E_{\mathrm{B},3}}, \tag{9}$$

$$k_{24} = \nu_2\,\mathrm{e}^{-\beta(E_{\mathrm{B,f}} - \gamma F)}, \text{ and } k_{42} = \nu_2\,\mathrm{e}^{-\beta(E_{\mathrm{B,r}} + \gamma F)}, \tag{10}$$

where the corresponding attempt frequencies and barriers are referred to as ν_i and $E_{\mathrm{B},i}$. The term γF represents the rise or the lowering of the barrier due to the applied electric field.

So far, only classical calculations of the band edge energy diagram have been performed to obtain the interface quantities, in particular the position of the band edges (E_{C}, E_{V}), the Fermi level (E_{F}), and the electric field (F) within the dielectric. These quantities enter the expressions of the rates and will alter them significantly due to their exponential dependences. Equations (6) are valid for a three-dimensional electron gas [4], however, this assumption breaks down for an inversion layer of MOS structures. In the one-dimensional triangular potential well at the interface, bound states build up

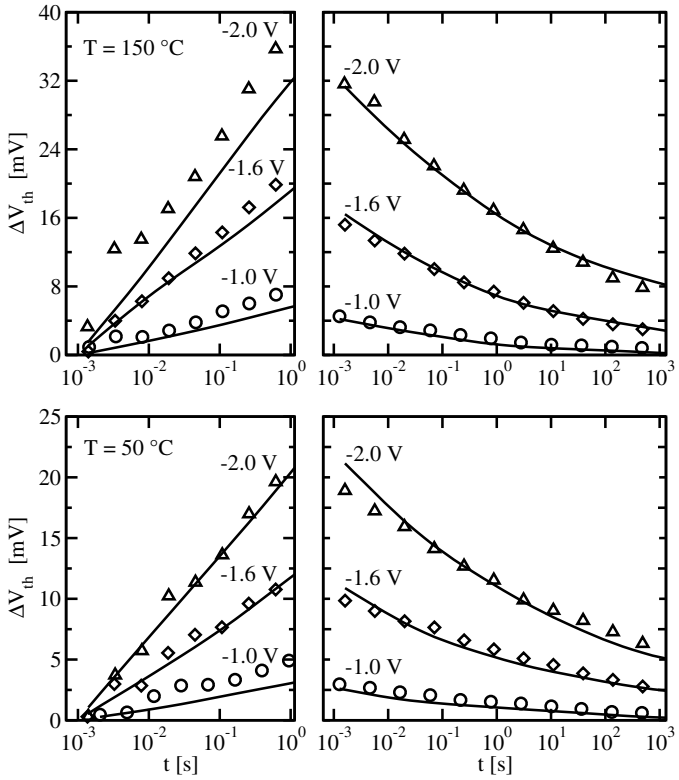

Fig. 4. Temporal evolution of the trapped charges neglecting quantization effects. A pMOSFET with a gate thickness of $1.75\,\mathrm{nm}$ is subjected to two different temperatures ($50\,^{\circ}\mathrm{C}$ upper panels, $150\,^{\circ}\mathrm{C}$ lower panels) and three different gate voltages for $1\,\mathrm{s}$ (-1.0, -1.6, $-2.0\,\mathrm{V}$) during the first phase termed trapping/stress (left hand side). After the gate voltage is removed, the second phase called detrapping/relaxation phase (right hand side) sets in. Symbols mark measurement data while solid lines belong to simulation data. Note that the temperature and field dependence is well reproduced simultaneously for relaxation phase. The slight tendency of the simulations to underestimate the measurements at high stress temperatures during the stress phase may be traced back to the mobility degradation of the drain current during the MSM measurements [8].

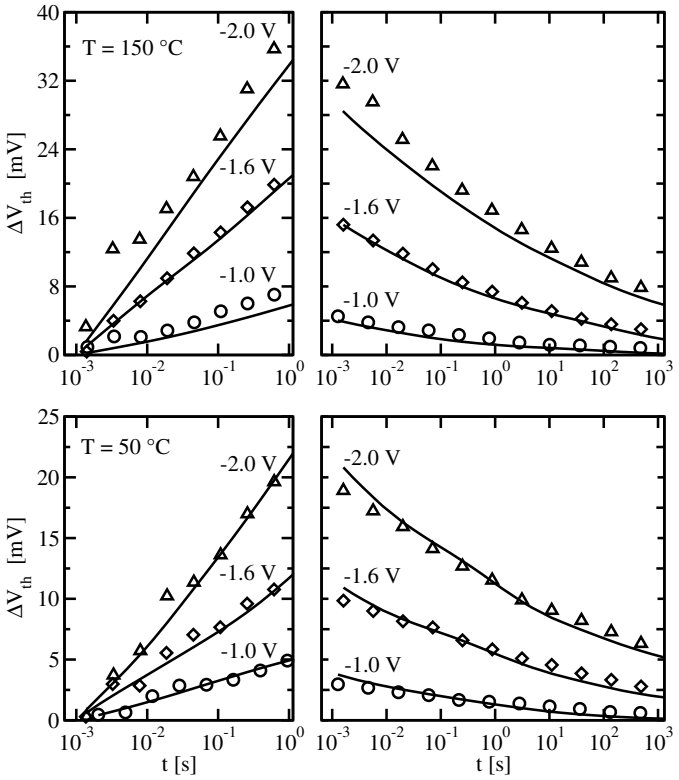

Fig. 5. The same as in Fig. 4 but for the quantum mechanical simulation. Again, very good agreement between recorded data and simulation data has been achieved.

and form subbands which correspond to the new initial or final energy levels for MPFAT transitions. For instance, electrons are energetically located in the bound states, which are situated above the conduction band edge and correspond to the new source of electrons in the respective rate expressions. With an increase in the applied gate bias, those bound states shift away from the conduction band which gives rise to different bias dependences (see Fig. 3).

III. Simulation and Results

We have performed numerical simulations on a pMOSFET structure with a $1.75\,\mathrm{nm}$ thick silicon oxynitride layer and an n-polygate. Due to the amorphous nature of silicon dioxide, a broad range of the electron energy levels and barriers must be expected. Defect levels and barriers associated with MPFAT trapping or detrapping processes are assumed to be homogeneously distributed while thermal barriers are taken to follow a Fermi-Derivative (Gaussian-like) distribution [9]. A large number of representative traps have been generated where each of them has an individual set of random energy levels and barriers. For the classical or quantum mechanical calculation of the bandstructure, a self-consistent Schrödinger Poisson solver [10] has been applied that delivers the carrier concentrations, the band edge energies, the subbands, the Fermi level, and the electric field across the dielectric for the evaluation of the trapping rates. For each representative trap, the respective set of rate equations is solved numerically. The resulting threshold voltage shift is obtained by averaging over the occupations of state 2 and state 4.

For comparison, we first applied the classical variant of the trapping model to experimental data shown in Fig. 4. One can clearly recognize that good agreement with experimental data is achieved for two temperatures and three different gate voltages. The parameter values assumed in the simulations are listed on Table I. Note that the model has to satisfy the following three criteria to explain measurement data: First, the evolution of trapped charges follows a logarithmic time behavior for the early part of the stress phase as well as for the early part of the relaxation phase. Second, the slopes of the stress and the relaxation phase exhibit a certain ratio (~ 2.5 in the lin-log plots), which goes hand in hand with the fact that detrapping phase spans over a much larger time range compared with the preceding trapping phase. Third, the experimental data exhibits an approximately quadratic temperature and field dependence [1].

The trapping model including quantization effects has been applied to the same set of experimental data. For a proper comparison to the classical variant of the trapping model, only

TABLE I

VALUES USED FOR THE CLASSICAL (LEFT COLUMN) AND THE SUBBAND (RIGHT COLUMN) MODEL. ENERGY DISTRIBUTIONS ASSOCIATED WITH LRME TRANSITIONS ARE ASSUMED TO BE HOMOGENEOUS. NOTE THAT THE TRAP ENERGY LEVELS ARE REFERENCED TO THE SUBSTRATE VALENCE BAND. FOR SIMPLICITY, THE INITIAL ($V_{\mathrm{I}} = 0.0\,\mathrm{eV}$) AND THE FINAL ($V_{\mathrm{F}}$) VALUE OF THE TRANSITION $2 \leftrightarrow 4$ ARE TAKEN TO BE SINGLE-VALUED, WHILE THE ENERGY BARRIERS V_{B} ARE DISTRIBUTED FOLLOWING A FERMI-DERIVATIVE. ONLY A FRACTION ($C = 0.12$) OF ALL TRAPS IS ALLOWED TO UNDERGO THIS TRANSITION. NOTE THAT THE ATTEMPT FREQUENCY ν_2 SHOWS AN TEMPERATURE DEPENDENCE.

k_{12}		
σ_n	$1.08 \times 10^{-15}\,\mathrm{cm}^2$	$1.08 \times 10^{-15}\,\mathrm{cm}^2$
σ_p	$1.24 \times 10^{-14}\,\mathrm{cm}^2$	$1.24 \times 10^{-14}\,\mathrm{cm}^2$
$E_{\mathrm{T,min}}$	$-1.14\,\mathrm{eV}$	$-1.64\,\mathrm{eV}$
$E_{\mathrm{T,max}}$	$-0.31\,\mathrm{eV}$	$-0.6\,\mathrm{eV}$
$E_{\mathrm{B,min}}$	$0.01\,\mathrm{eV}$	$0.03\,\mathrm{eV}$
$E_{\mathrm{B,max}}$	$1.15\,\mathrm{eV}$	$1.04\,\mathrm{eV}$
F_{c}	$2.83\,\mathrm{MV/cm}^2$	$3.66\,\mathrm{MV/cm}^2$
k_{23} and k_{32}		
σ_n	$1.08 \times 10^{-15}\,\mathrm{cm}^2$	$1.08 \times 10^{-15}\,\mathrm{cm}^2$
σ_p	$1.24 \times 10^{-14}\,\mathrm{cm}^2$	$1.24 \times 10^{-14}\,\mathrm{cm}^2$
$E_{\mathrm{T,min}}$	$0.01\,\mathrm{eV}$	$-0.35\,\mathrm{eV}$
$E_{\mathrm{T,max}}$	$0.3\,\mathrm{eV}$	$0.63\,\mathrm{eV}$
F_{c}	none	none
k_{31}		
$\nu_{2,50\mathrm{C}}$	$5.11 \times 10^{15}\,1/\mathrm{s}$	$5.11 \times 10^{15}\,1/\mathrm{s}$
$\nu_{2,150\mathrm{C}}$	$3.54 \times 10^{10}\,1/\mathrm{s}$	$3.5 \times 10^{10}\,1/\mathrm{s}$
$V_{\mathrm{B,m}}$	$1.46\,\mathrm{eV}$	$1.46\,\mathrm{eV}$
$V_{\mathrm{B,s}}$	$0.44\,\mathrm{eV}$	$0.44\,\mathrm{eV}$
V_{F}	$0.0\,\mathrm{eV}$	$0.0\,\mathrm{eV}$
γ	$0.74\,\mathrm{nm}$	$0.74\,\mathrm{nm}$
k_{24} and k_{42}		
ν_1	$10^{13}\,1/\mathrm{s}$	$10^{13}\,1/\mathrm{s}$
$E_{\mathrm{B,min}}$	$0.01\,\mathrm{eV}$	$0.01\,\mathrm{eV}$
$E_{\mathrm{B,max}}$	$1.15\,\mathrm{eV}$	$1.15\,\mathrm{eV}$

the LRME parameters have been optimized while other all other parameters were held fixed. As shown in Fig. 5, the simulation shows very good agreement with experimental data reproducing the field- as well as the temperature dependence. Mind that the uppermost trap level E_{T} has been shifted downwards (Table I) in energy by about the same energy as the separation of the trap level from the conduction band edge (ranging between 169 and 277 meV). Since the changes in the occupancy in the states 3 and 4, the major fraction of injected holes into the dielectric will end up in states 2. Thus the field- and temperature dependence can be ascribed to the increase of the rates from states 1 into state 2 as demonstrated in Fig. 6. Due to the shift of the first subband and the field enhancement the factor rates increase with higher gate voltages, while higher temperatures raise the probabilities to overcome the LRME barriers.

IV. CONCLUSION

We have refined a recently published charge trapping model accounting for quantization effects. The consideration of subbands should affect the trapping dynamics as well as the extent of the field-acceleration. However, the required qualitative behavior, such as field- and temperature-acceleration along with the experimentally observed time scales covered by trapping and detrapping phase, are preserved. Nevertheless, a shift in the extracted model parameters, regarding the energy trap levels and the LRME barriers, has been observed.

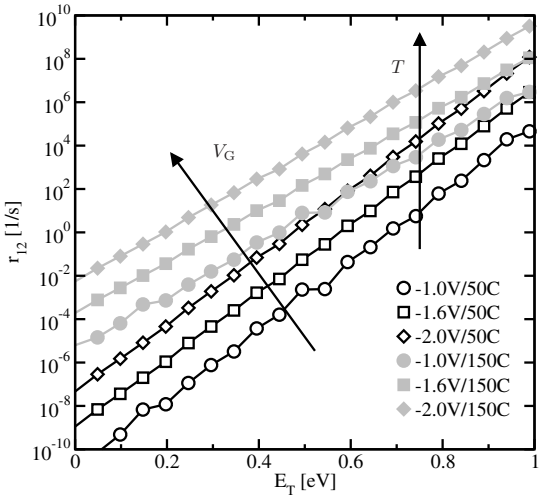

Fig. 6. Rates from state 1 into state 2 as a function of the trap levels E_{T} in state 1 (referred to the lowest trap). Due to the fact that nearly all injected charges accumulate in state 2, the injection rates are determined by the dependence of k_{12} on temperature and the electric field.

REFERENCES

[1] T. Grasser, B. Kaczer, W. Goes, T. Aichinger, P. Hehenberger, and M. Nelhiebl, "A Two-Stage Model for Negative Bias Temperature Instability," in *Proc. Intl.Rel.Phys.Symp.*, 2009, pp. 33–44.

[2] A. Lelis and T. Oldham, "Time Dependence of Switching Oxide Traps," *IEEE Trans.Nucl.Science*, vol. 41, no. 6, pp. 1835–1843, Dec 1994.

[3] R. Siergiej, M. White, and N. Saks, "Theory and Measurement of Quantization Effects on $\mathrm{Si-SiO_2}$ Interface Trap Modeling," *Solid-State Electron.*, vol. 35, no. 6, pp. 834–854, 1992.

[4] N. Zanolla, D. Siprak, P. Baumgartner, E. Sangiorgi, and C. Fiegna, "Measurement and Simulation of Gate Voltage Dependence of RTS Emission and Capture Time Constants in MOSFETs," in *Ultimate Integration of Silicon*, 2008, pp. 137–140.

[5] M. Kirton and M. Uren, "Noise in Solid-State Microstructures: A New Perspective on Individual Defects, Interface States and Low-Frequency (1/f) Noise," *Adv.Phys*, vol. 38, no. 4, pp. 367–486, 1989.

[6] S. Makram-Ebeid and M. Lannoo, "Quantum Model for Phonon-Assisted Tunnel Ionization of Deep Levels in a Semiconductor," *Physical Review B*, vol. 25, no. 10, pp. 6406–6424, 1982.

[7] S. Ganichev, W. Prettl, and I. Yassievich, "Deep Impurity-Center Ionization by Far-Infrared Radiation," *Phys.Solid State*, vol. 39, no. 1, pp. 1703–1726, 1997.

[8] B. Kaczer, T. Grasser, P. Roussel, J. Martin-Martinez, R. O'Connor, B. O'Sullivan, and G. Groeseneken, "Ubiquitous Relaxation in BTI Stressing-New Evaluation and Insights," in *Proc. Intl.Rel.Phys.Symp.*, 2008, pp. 20–27.

[9] A. Haggag, W. McMahon, K. Hess, K. Cheng, J. Lee, and J. Lyding, "High-Performance Chip Reliability from Short-Time-Tests," in *Proc. Intl.Rel.Phys.Symp.*, 2001, pp. 271–279.

[10] M. Karner, A. Gehring, S. Holzer, M. Pourfath, M. Wagner, W. Goes, M. Vasicek, O. Baumgartner, C. Kernstock, K. Schnass, G. Zeiler, T. Grasser, H. Kosina, and S. Selberherr, "A Multi-Purpose Schrödinger-Poisson Solver for TCAD Applications," *J. Comput. Electronics*, vol. 6, pp. 179–182, 2007.